ECONTECHMOD. AN INTERNATIONAL QUARTERLY JOURNAL – 2017, Vol. 06, No. 3, 105–110

A mathematical method for modeling the shape of apples Part 2. Calculation and validation of results

L. Mieszkalski, J. Wojdalski

Department of Production Management and Engineering,
Warsaw University of Life Sciences, Nowoursynowska 166, 02-787 Warsaw, Poland
leszek_mieszkalski@sggw.pl; janusz_wojdalski@sggw.pl

Received: February 25, 2017; Accepted: May 15, 2017

Summary. The aim of the study was to propose a mathematical method for modeling the shape of apples cv. *Ligol* and their anatomical parts, the locule and the pericarp, with the use of Bézier curves. The method developed in part 1 of the study was used to generate 3D models describing the shape of an apple, the locule and the pericarp. The main projection planes of the apple, locule and pericarp were compared with their corresponding models to reveal that the proposed method supports modeling of geometric solids with sufficient accuracy for practical applications.
Key words: apple, cv. *Ligol*, locule, pericarp, shape, 3D model, validation.

INTRODUCTION

This article is a continuation of the research undertaken by Mieszkalski and Wojdalski [1].Ki et al. [2] relied on the finite element method (FEM) to examine the mechanical properties of apples in a 3D model. The 3D model of an apple was generated in several steps. The coordinates of points on the surface of the apple were measured, and the results were used to generate a mesh on the apple's surface. In the following step, data were smoothed. A 3D model of an apple comprising 30,000 finite elements was subjected to a strength analysis. According to Anand and Scanlon [3], strength analyses of fruit are difficult to perform due to the anisotropic structure and complex shape of the examined objects. Bartoň et al. [4] described the shape of a biological object by measuring the coordinates of pixels along the object's circumference, where the least squares methods was used to reduce the number of pixels. According to Bartoň [5], photographs in three projections (main projection, from the left, from the top) and approximation procedures facilitate modeling. Rogge et al. [6] developed a geometric model of an apple based on computed tomography (CT) scans. The shape of the fruit was described by elliptical Fourier analysis, and new apple shapes were randomly generated in a statistical analysis. 3D models of apples were used in strength analyses with the involvement of the finite element method. Mieszkalski [7] used Bézier curves to describe the external surface of an apple. Mendoza et al. [8] proposed a method for 3D representation of the microstructure of apples based on CT scans. The spatial distribution of pores in apple tissue is an important consideration when describing complex transportation processes in apples. Jancsók et al. [9] conducted strength analyses of apples and pears based on 3D models developed from photographic images of object segments, image analyses with edge detection, curve rotation by a preset angle, and the finite element method. Rome [10] calculated the pressure at which mechanical damage is inflicted on apples at various packing densities. 3D models describing the shape of apples are subjected to static and dynamic tests with the involvement of the finite element method. The finite element method was also applied to calculate heat flow in strawberries with the use of 3D scanning in the SolidWorks program (CAD software) [11]. Bubeníčková et al. [12] described the shape of potato tubers based on photographs, and they described potato contours with the use of pole coordinates and Fourier methods. According to Costa et al. [13] and Prabha and Kumar [14], fruits are graded and sorted based mainly on their shape. Machine vision and image analysis techniques are deployed to control the quality, color and shape of the processed objects. Fruits have irregular shape which can be described with the use of boundary descriptors. Ohali [15] proposed a fruit sorting system based on machine vision. Kavdır and Guyer [16] analyzed image recognition methods in apple sorting systems. Defects in graded and sorted apples are detected with the use of vision systems [17]. Ibrahim et al. [18] described the shape of mango fruits with the use of elliptical Fourier

analysis to eliminate incorrectly shaped fruits during sorting.

The aim of this study was to develop a 3D model describing the shape of an apple, its pericarp and locule with the use of the method proposed in part 1 of the study [1].

MATERIALS AND RESULTS

The study was performed on apples cv. *Ligol* characterized by spherical and conical shape. Photographs of an unbruised apple, selected from a batch of 50 fruits, are presented in Figure 1 in part 1 of the study.

In the mathematical model proposed in part 1 [1], the coordinates of points on the surface of the apple are written in a matrix. The model relies on Bézier curves to describe the shape of the apple, its locule and pericarp. Apples have concave and convex surfaces, therefore, three smooth-joined Bézier curves were used to model the contour of the analyzed fruit. The initial point (node) of a Bézier curve is positioned inside the lower part of the pedicel cavity. The first Bézier curves (a total of 10 curves) plotted from that point describe the shape of an apple's pedicel cavity. The second nodes of the first Bézier curves are connected to the nodes of the second Bézier curves describing the middle part of the apple which is a convex surface. The points at which the curves intersect are smoothed. The second nodes of the second Bézier curves are connected to the first nodes of the third Bézier curves describing the shape of the calyx basin. The second nodes of the third Bézier curves meet in the apex of the calyx basin. The nodes at the bottom of the pedicel cavity and the apex of the calyx basin are determined by the values of parameters h_1 and h_2 presented by Mieszkalski and Wojdalski [1] (Fig. 2 and Table 1). When determining the shape of the three joined Bézier curves, the second nodes of the first Bézier curves, the first nodes of the second Bézier curves, and the first nodes of the third Bézier curves have to be positioned on the meridians of the modeled surface. The external surface of the locule and the external surface of the pericarp were described with two smooth-joined Bézier curves each. The nodes and control points of those Bézier curves are presented in Figure 5 in part 1 of the study.

The accuracy of a 3D model of an apple cv. *Ligol*, the locule and the pericarp was determined by calculating the difference in the distance (mm) between the edge of the apple, the locule and the pericarp, and the edges of their corresponding models in the main projection planes in the *Inkscape* program.

RESULTS

A single contour of the modeled apple (three joined Bézier curves) was mapped with four nodes and six control points. The coordinates of 40 nodes and 60 control points have to be changed to modify the shape of 10 contours positioned at 36° intervals along the apple's surface (Fig. 4, Tables 1 and 2 in part 1 of the study [1]).

Table 1. Coordinates of nodes in pedicel cavities and calyx basins of the modeled apple

Nodes in the pedicel cavity and the calyx basin	Node coordinates [mm]
Ax	0
Ay	0
Az	69.7
Cx	0
Cy	0
Cz	15.4

Table 2. Coordinates of nodes and control points of Bézier curves for ten contours of the modeled apple cv. *Ligol*

Control points and nodes	Number of curve (n)									
	1	2	3	4	5	6	7	8	9	10
Anx	-7.2	-7.4	-8.4	-8.1	-8.2	-1.1	1.9	1.9	1.6	1.9
Any	-7.2	-7.4	-8.4	-8.1	-8.2	-1.1	1.9	1.9	1.6	1.9
Any	83.6	83.2	84.6	84.7	84.9	83.2	82.9	82.9	83.2	82.8
AAnx	-26	-26.7	-28	-27.9	-25.5	18.7	18.7	18.7	18.6	18
AAny	-26	-26.7	-28	-27.9	-25.5	18.7	18.7	18.7	18.6	18
AAnz	78.2	78.3	78.2	78.1	78.5	83	81.2	81.1	80.9	81.1
ABnx	-31.2	-31.7	-32.8	-33.3	-31.2	29.4	28	27.6	27	27
ABny	-31.2	-31.7	-32.8	-33.3	-31.2	29.4	28	27.6	27	27
ABnz	73.5	73.5	73.5	73.5	73.5	73.5	73.5	73.5	73.5	73.5
BCnx	-35.3	-38	-38.5	-34.5	-30.7	29.6	27.3	27.1	25.4	25.5
BCny	-35.3	-38	-38.5	-34.5	-30.7	29.6	27.3	27.1	25.4	25.5
BCnz	11.5	11.5	11.5	11.5	11.5	11.5	11.5	11.5	11.5	11.5
Bnx	-51.2	-55.6	-56.4	-56.5	-54.4	41.2	38.6	38.9	37.6	42.8
Bny	-51.2	-55.6	-56.4	-56.5	-54.4	41.2	38.6	38.9	37.6	42.8

Bnz	55.2	51.6	51.9	51.8	51.8	62.3	63.5	63.1	61.7	56.8
BBnx	-49.5	-47.8	-46.2	-43.4	-39.8	46.2	41.8	43.2	41.2	41
BBny	-49.5	-47.8	-46.2	-43.4	-39.8	46.2	41.8	43.2	41.2	41
BBnz	22.4	23.9	24.3	24.4	24.4	37.6	34.5	35.2	35.7	35
CCnx	-31.2	-33.9	-32.2	-31.7	-28	19.5	17.6	18.1	16.3	16
CCny	-31.2	-33.9	-32.2	-31.7	-28	19.5	17.6	18.1	16.3	16
CCnz	4.1	4.6	4.8	6.2	6.4	-2.2	-3.1	-1.4	-2	-1.7
Cnx	-13.1	-13.7	-12.3	-12.5	-12.2	-0.5	-0.9	-0.4	-0.5	-0.9
Cny	-13.1	-13.7	-12.3	-12.5	-12.2	-0.5	-0.9	-0.4	-0.5	-0.9
Cnz	-10.1	-5.9	-2.4	-2.5	-2.7	-3.4	-3.1	-3.3	-5.3	-5.5

A 3D model of an apple (Fig. 1) was developed based on the proposed mathematical model and the data presented in Tables 1 and 2.

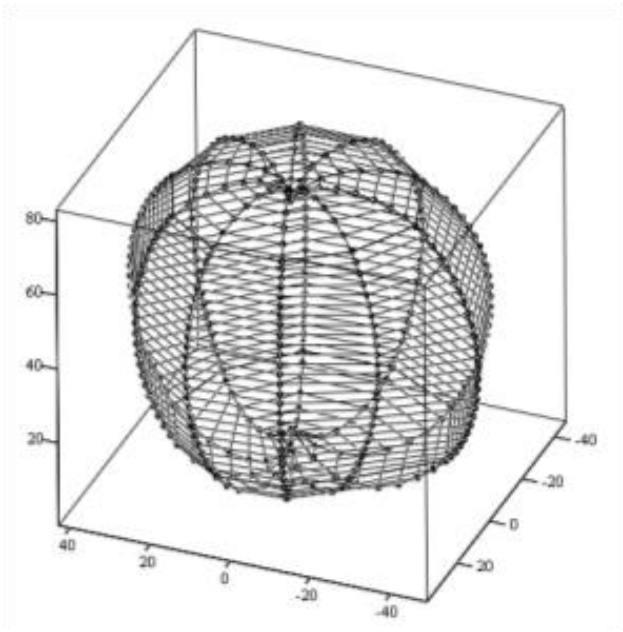

Fig. 1. A 3D model of an apple cv. *Ligol*

The shape of the locule and the pericarp is modeled by rotating the contour composed of two smooth-joined Bézier curves. The position of locule apex points on the side of the pedicel cavity is determined by the first node of the first Bézier curves. The position of locule apex points on the side of the calyx basin is determined by the third node of the second Bézier curves. The first and second Bézier curves are connected at points where the first Bézier curves end and the second Bézier curves begin.

The position of locule and pericarp apexes is determined by the values of parameters h_1 and h_2 presented in part 1 of the study [1] (Fig. 2, Table 1). Three nodes and four control points are used to change the shape of the locule and the pericarp (Tables 1 and 3).

Table 3. Coordinates of nodes and control points of the locule and the pericarp of the modeled apple

Control points and nodes	Locule	Pericarp
*A*1*x*	0	0.3
*A*1*z*	65.5	62.4
*B*1*x*	1	2.8
*B*1*z*	61.3	56.3
Bx	8.1	7.1
Bz	53.7	50.9
*B*2*x*	16.3	11.6
*B*2*z*	42.1	41.5
*C*1*x*	2.5	1
*C*1*z*	24.2	30.3

3D models of the modeled apple's locule and the pericarp (Fig. 2) were developed based on the proposed mathematical model and the data presented in Tables 1 and 3.

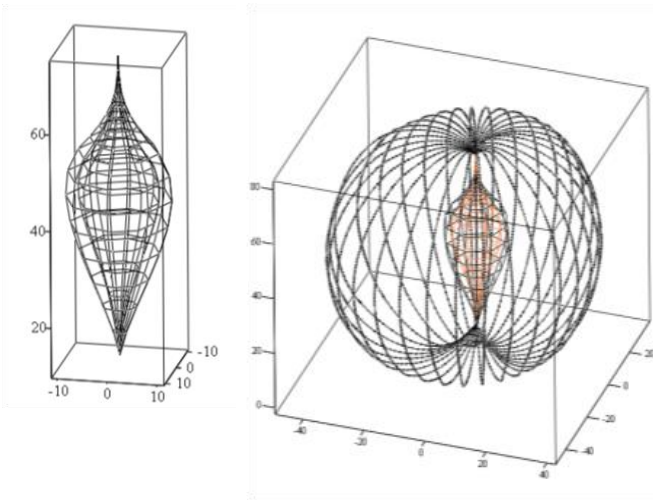

Fig. 2. A 3D model of an apple's locule and pericarp and a 3D model of an apple cv. *Ligol* with the locule and the pericarp

VALIDATION

The three main projection planes of an apple cv. *Ligol*, its locule, pericarp and their corresponding 3D models are overlaid in Figure 3. The differences in the distance (mm) between the edges of the apple, locule, pericarp, and the edges of their corresponding models in the main projection planes are presented in Table 4.

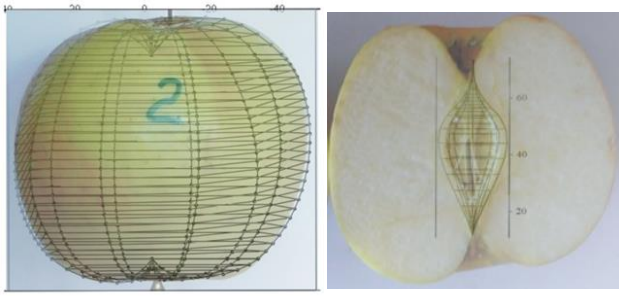

Fig. 3. A comparison of an apple cv. *Ligol*, its locule and pericarp with their corresponding 3D models.

Table 4. Differences in the distance (mm) between the edges of an apple, locule and pericarp, and the edges of their respective models in the main projection planes

Measurement in the main projection plane (mm)	Difference in distance (mm)
Apple	
1.5	4.1
10.8	0.8
18.5	1.1
22.8	0.9
39.9	1.1
66.5	1.5
74.4	1.7
72.2	1.3
77.2	3.4
78.1	0.2
Locule	
25.6	0.5
29.7	0.7
53.6	1.4
56.9	2.2
Pericarp	
33.5	0.4
36.3	0.8
39.7	1.2
42.4	0.1

The differences in the distance (mm) between the edges of the apple and the edges of the model in the main projection plane range from 0.1 to 1.7 mm and, locally along a short section, from 3.4 to 4.1 mm. These minor differences indicate that the developed 3D model provides a good fit to the external surface of the apple. The differences in the distance (mm) between the edges of the apple's locule and the edges of the model in the main projection plane range from 0.5 to 2.2 mm and between the edges of the pericarp and the edges of the model – from 0.1 to 1.2 mm. These minor differences also suggest that the 3D model provides a good fit to the apple's locule and pericarp.

CONCLUSIONS

The proposed mathematical method for modeling the shape of an apple, its locule and pericarp renders the external surface of apples and their anatomical parts with sufficient accuracy for practical applications. The differences in the distance (mm) between the edges of the apple, its locule and pericarp, and the edges of their corresponding models in the main projection planes were small in the range of 0.1 to 4.1 mm. The results of this study can be used to design innovative solutions for packaging apples or detecting bruised fruits [see for instance 19-22].

REFERENCES

1. **Mieszkalski L. &Wojdalski J., 2017**. A mathematical method for modeling the shape of apple.Part 1. description of the method. ECONTECHMOD. An International Quarterly Journal
2. **Kim G-W. Do G-S. Bae Y.&Sagara Y., 2008.**Analysis of Mechanical Properties of Whole Apple Using Finite Element Method Based on Three-Dimensional Real Geometry. Food Sci. Technol. Res., 14 (4), 329-336.
3. **Anand A. & Scanlon M.G.,2002**. Dimensional effects on the prediction of texture-related mechanical properties of foods by indentation. Trans. of the ASAE, 45, 1045-1050.
4. **Bartoň S. Severa L. &Buchar J.,2010.**New algorithm for biological objects' shape evaluation and data reduction. ActaUniversitatisAgriculturae et SilviculturaeMendelianaeBrunensis, LVIII 1, 1, 13-20.
5. **Bartoň S., 2008.** Three dimensional modelling of the peach in Maple. In: CHLEBOUN, J. Programs and Algorithms of numerical Mathematics. 1st ed. Praha. Matematickýústav AV ČR; 7-14. ISBN 978-80-85823-55-4.
6. **Rogge S. Beyene S. Herremans E. Defraeye T. Verboven P. &Nicolai B., 2013.** A geometrical model generator for quasi-axisymmetric fruit. Proceedings of the 7th International Conference on

Functional-Structural Plant Models, Saariselkä, Finland, 9-14 ,June 2013. Eds. RistoSievänen, EeroNikinmaa, Christophe Godin, Anna Lintunen & Pekka Nygren. 92-94. http://www.metla.fi/fspm 2013/proceedings. ISBN 978-951-651-408-9.

7. **Mieszkalski L., 2015**. Komputerowe wspomaganie modelowania kształtu jabłek. Acta Sci. Pol. TechnicaAgraria, 14(3-4), 19-31.
8. **Mendoza F., Verboven P., Ho Q. T., Mebatsion H. K., Nguyen T. A., Wevers M. &Nicolaï B., 2006**. 3-D microscale geometry of apple tissue using X-ray computed microtomography. IUFoST 2006; 761-773, DOI: 10.1051/IUFoST:20060431.
9. **Jancsók P. Coucke P. Beuselinck A. De Baerdemaeker J.& Nicolai B., 1998.** 3D finite element model generation by computer vision for the modal analysis of fruits. Food quality modeling. Edited by: B. M. Nicolai, J. De Baerdemaeker; 139-144, ISBN 92-828-3309-7.
10. **Romo E. R., 2005.** An experimental, analytical and numerical analysis of apple bruising. bibing.us. es/proyectos/abreproy/3994/fichero/Thesis.pd. Data dostępu 05.12.2016.
11. **Uyar R. &Erdoğdu F., 2016.** Computational Modelling of Heat Transfer in Food Processes with 3-Dimensional Scanners [www.icef11.org/content/ papers/mcf/MCF280.pdf]. Data dostępu 05.12.2016.
12. **Bubeníčková A. Simeonovová J. Kumbár V. Jůzl M. &Nedomová Š., 2011**. Mathematical descriptive characteristics of potato tubers' shape. Acta Universitatis Agriculturae et Silviculturae Mendelianae Brunensis, LIX 8, 6, 63 - 67
13. **Costa, C., Antonucci, F., Pallattino, F., Aguzzi, J., Sun, D.W., &Menesatti, P. 2011.**Shape analysis of agricultural products: A review of recent research advances and potential application to computer vision. Food & Bioprocess Technology, 4, 673-692.
14. **Prabha D.S. & Kumar J. S., 2012.**A study on image processing methods for fruit classification. Proc. Int. Conf. on Computational Intelligence and Information Technology, CIIT, 403-406.
15. **Ohali Y. Al., 2011.** Computer vision based date fruit grading system: Design and implementation. Journal of King Saud University – Computer and Information Sciences, 23, 1, 29-36
16. **Kavdır I. & Guyer D.E., 2008.**Evaluation of different pattern recognition techniques for apple sorting. Biosystems Engineering, 99, 2, 211–219.
17. **Mehla P.M., Chenb Y-R., Kimb M. S., &Chan D. E., 2004.** Development of hyperspectral imaging technique for the detection of apple surface defects and contaminations. Journal of Food Engineering, 61, 1, 67-81.
18. **Ibrahim M. F., Sa'ad F. S. A., Zakaria A. & MdShakaff A.Y., 2016.** In-Line Sorting of Harumanis Mango Based on External Quality Using Visible Imaging. Sensors 2016, 16, 1753; 2-17 doi:10.3390/s16111753, http://www.mdpi.com/journal/sensors.
19. **Czernyszewicz E., 2008.** The importance of some selected qualitative features of apples for buyers (Ważność wybranych cech jakościowych jabłek dla konsumentów). ŻYWNOŚĆ. Nauka. Technologia. Jakość, 1 (56), 114-125.
20. **Flys I., 2014**. Conception of simulating the processes of innovative projects initialization for agro-industrial production in Ukraine. ECONTECHMOD. An International Quarterly Journal, 3, 4, 75-81.
21. **Gołacki K. Bobin G. &Stropek Z., 2009.**Bruise resistance of Apple (Melrose variety). TEKA Kom. Mot. Energ. Roln. – OL PAN, 9, 40-47
22. **Puchalski C. Gorzelany J. Zagula G.&Brusewitz G., 2008**. Image analysis for apple defect detection. TEKA Kom. Mot. Energ. Roln. – OL PAN, 8, 197-205.